Solar UV Spectroscopy and Coronagraphy

Werner Curdt

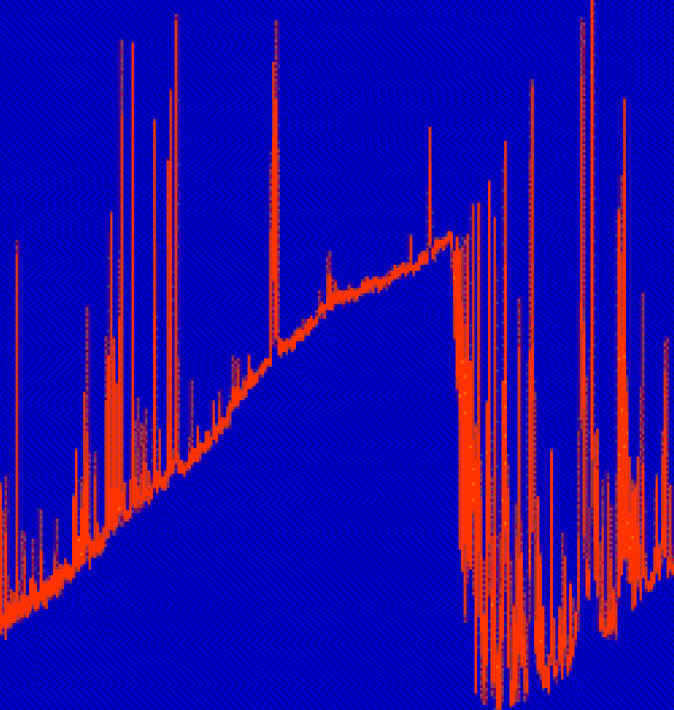

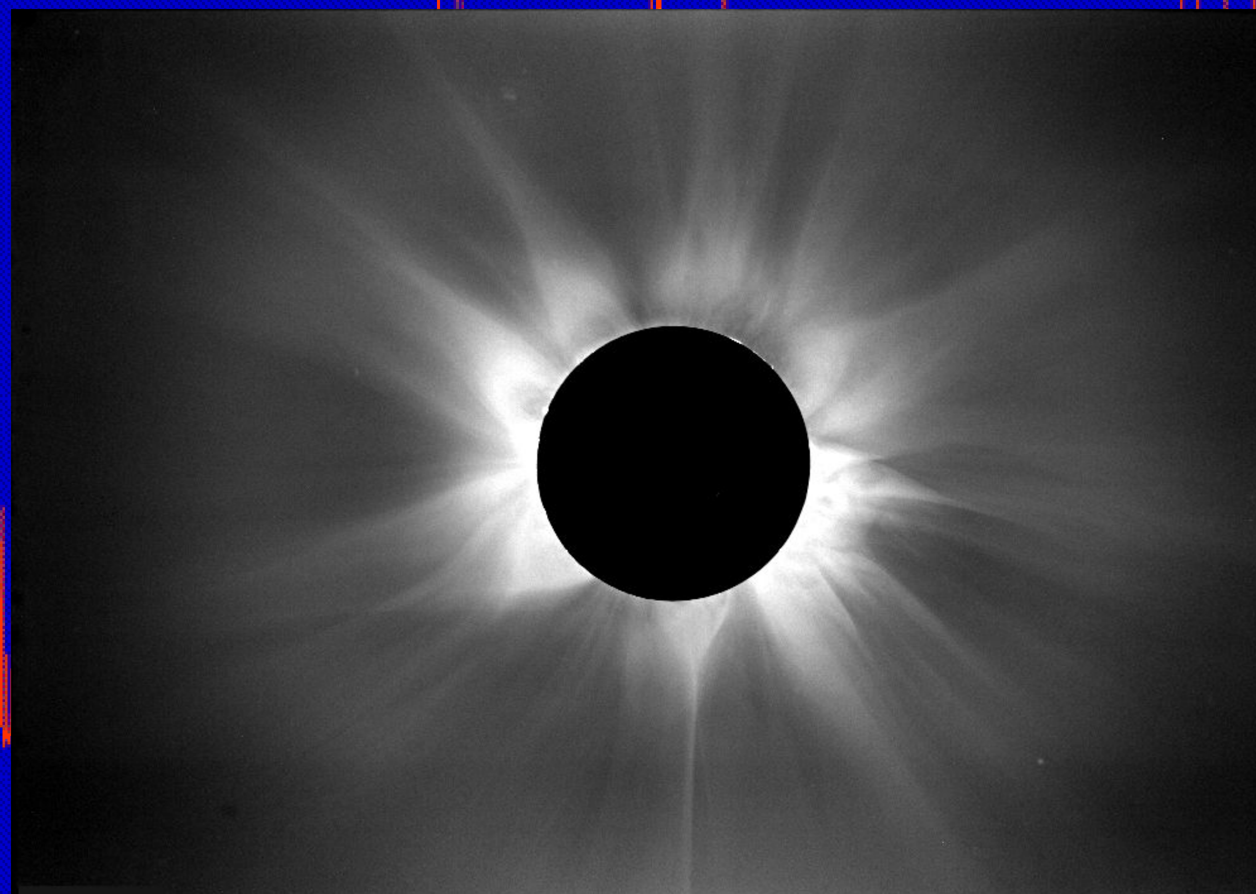

Outline

- motivation
  - the Sun‘s electromagnetic spectrum
  - spectroscopic methods
  - observational examples
- instrumental aspects
  - optical design
  - detectors
  - others
- highlights and outlook
- coronagraphy
  - the solar corona
  - instrumental aspects

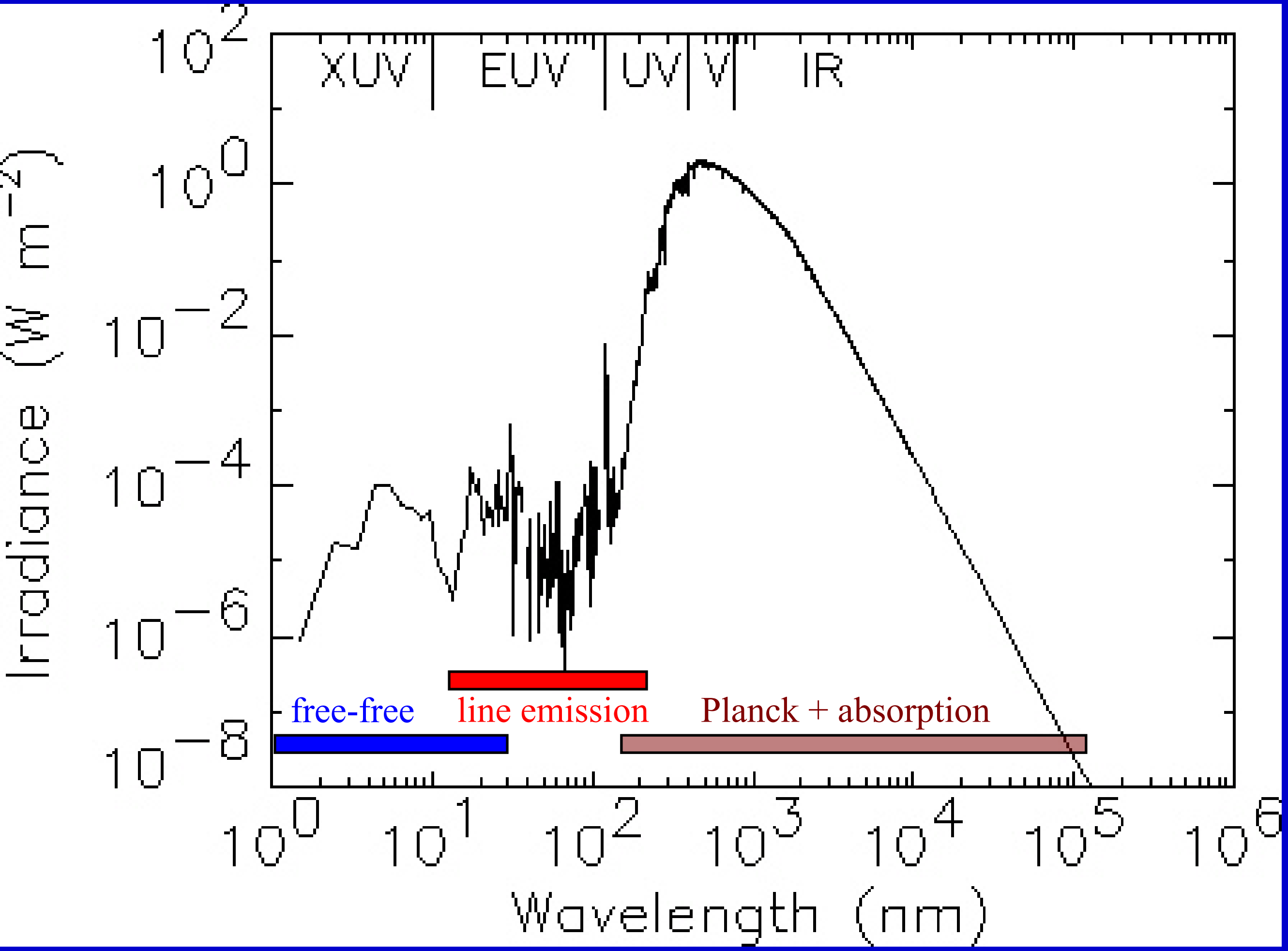

spectral categories:

XUV 0.1 – 10 nm
- HXR < 0.1 nm
- SXR 0.1 – 10

VUV 10 – 200 nm
- EUV 10 – 121
- FUV 121 – 200

MUV 200 – 300 nm
- UV- C 100 – 280

NUV 300 – 400 nm
- UV- B 280 – 315
- UV- A 315 – 400

VIS 380 – 760 nm

IR 760 nm – 1 mm

radio 1mm – 100 m

The solar irradiance spectrum above earth atmosphere (SOLAR2000)

transmission of the Earth atmosphere

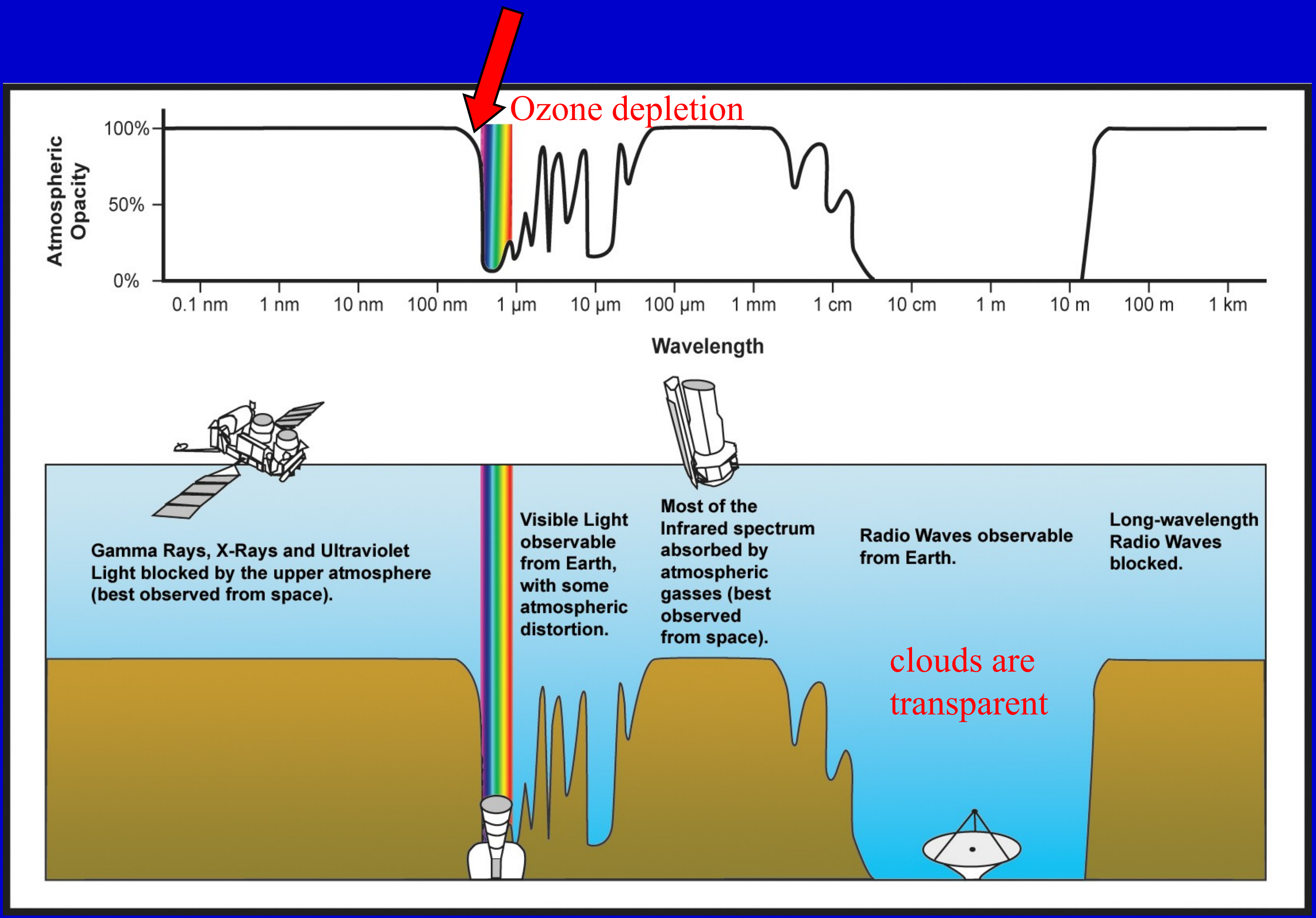

Spectroscopic methods

- line identification / selection
- line shifts / Doppler flows
- line widths / line shape
- plasma diagnostics / line ratios
- raster scans
- drift scans
- abundance measurements / FIP effect
- radiance / irradiance
- atomic physics

recombination continua:

> 1000 emission lines:

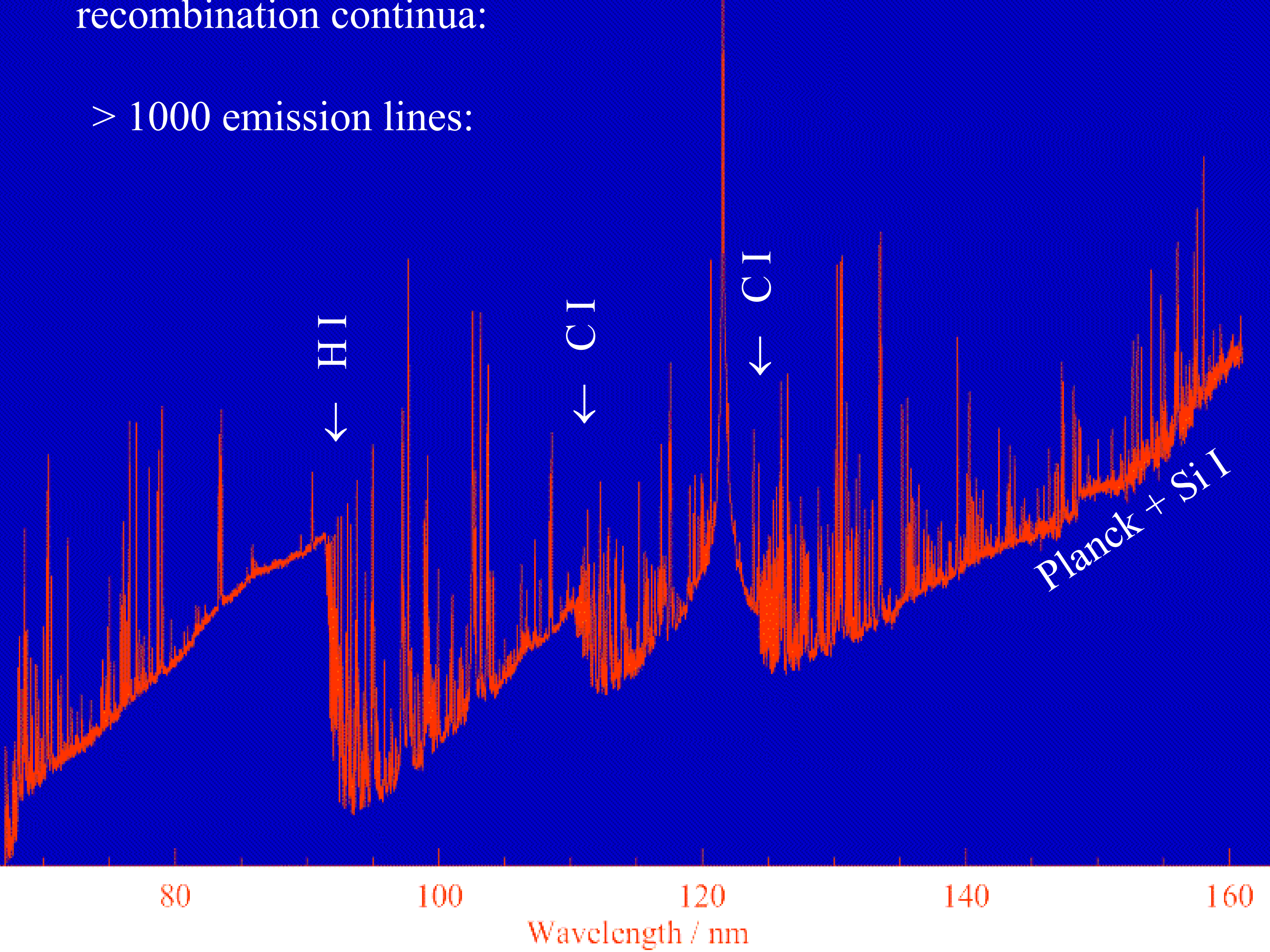

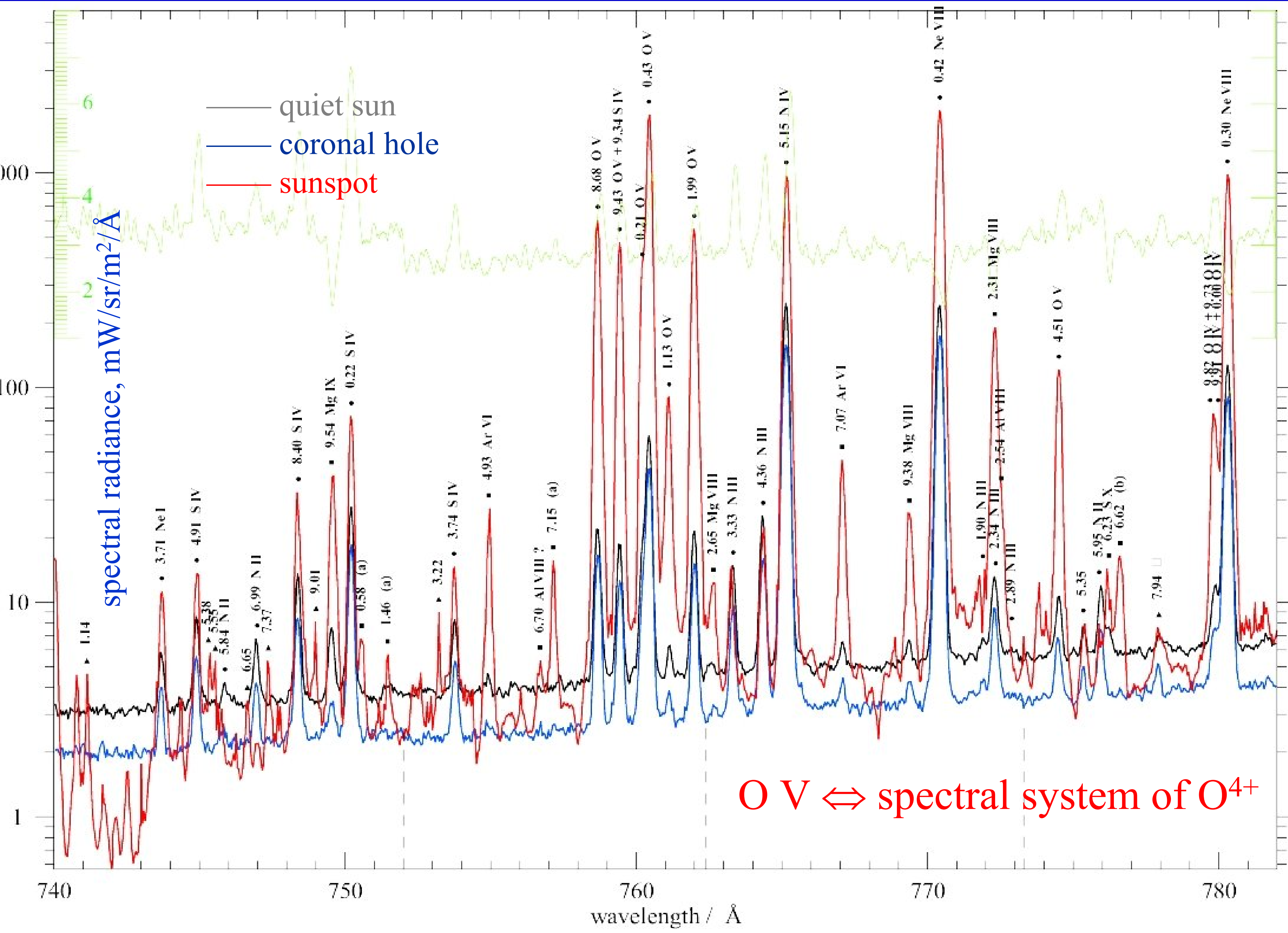
quiet sun
coronal hole
sunspot
spectral radiance, mW/sr/m²/Å
wavelength / Å
740
750
760
770
780
1
10
100
6
4
2
O V ⇔ spectral system of O4+
3.71 Ne I
4.91 S IV
8.40 S IV
9.54 Mg IX
0.22 S IV
3.74 S IV
4.93 Ar VI
6.70 Al VIII ?
7.15 (a)
8.68 O V
9.43 O V + 9.34 S IV
0.21 O V
0.43 O V
1.13 O V
1.99 O V
2.65 Mg VIII
3.33 N III
4.36 N III
5.15 N IV
7.07 Ar VI
9.38 Mg VIII
0.42 Ne VIII
1.90 N III
2.34 N III
2.31 Mg VIII
2.54 Al VIII
2.89 N III
4.51 O V
5.35
5.95 N II
6.23 S X
6.62 (b)
7.94
0.30 Ne VIII
6.99 N II
0.58 (a)
1.46 (a)
3.22
9.01
6.05
7.37
1.14

QUIET SUN EUV BRIGHTNESS COMPONENTS

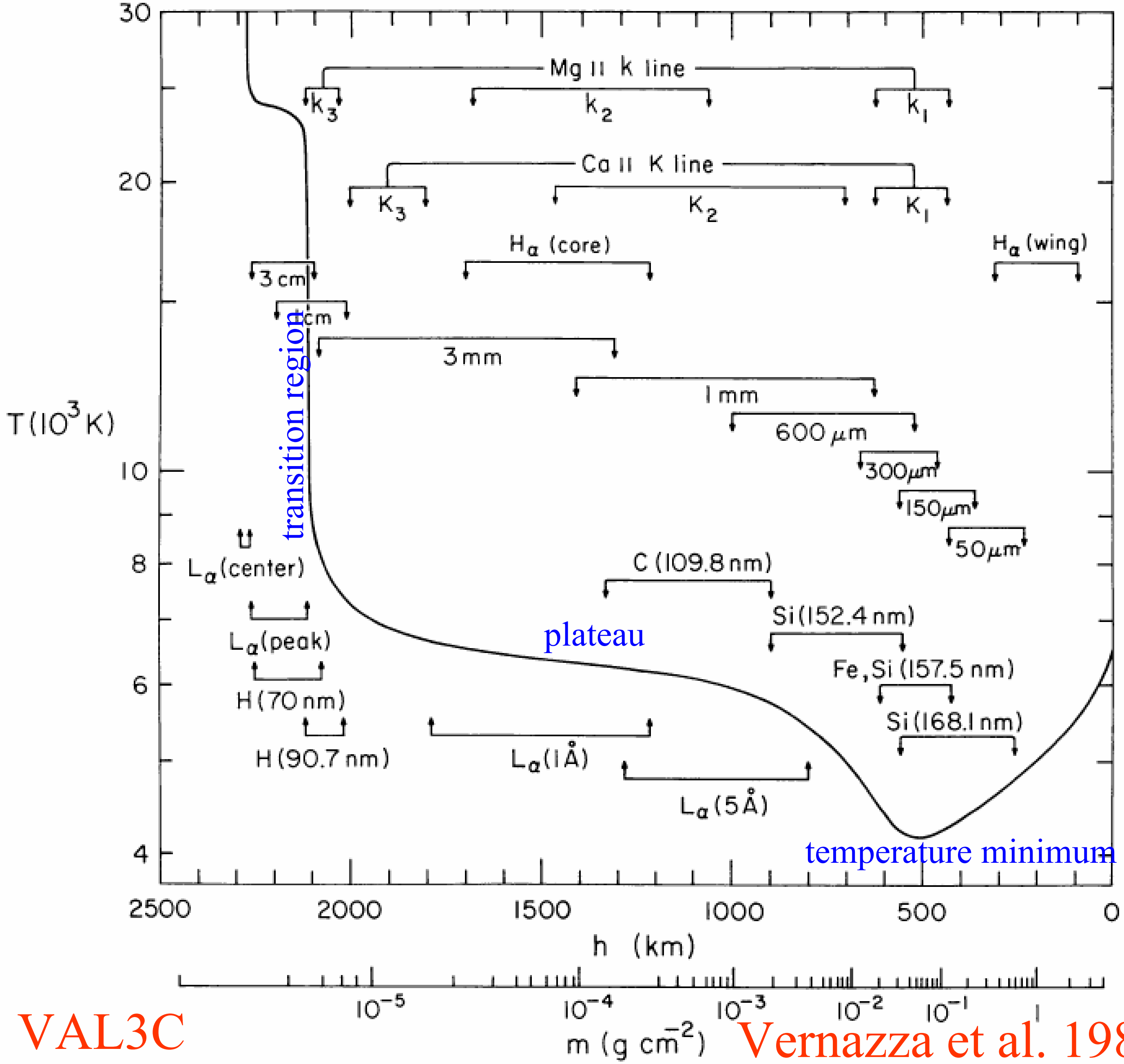

VAL3C

Vernazza et al. 1981

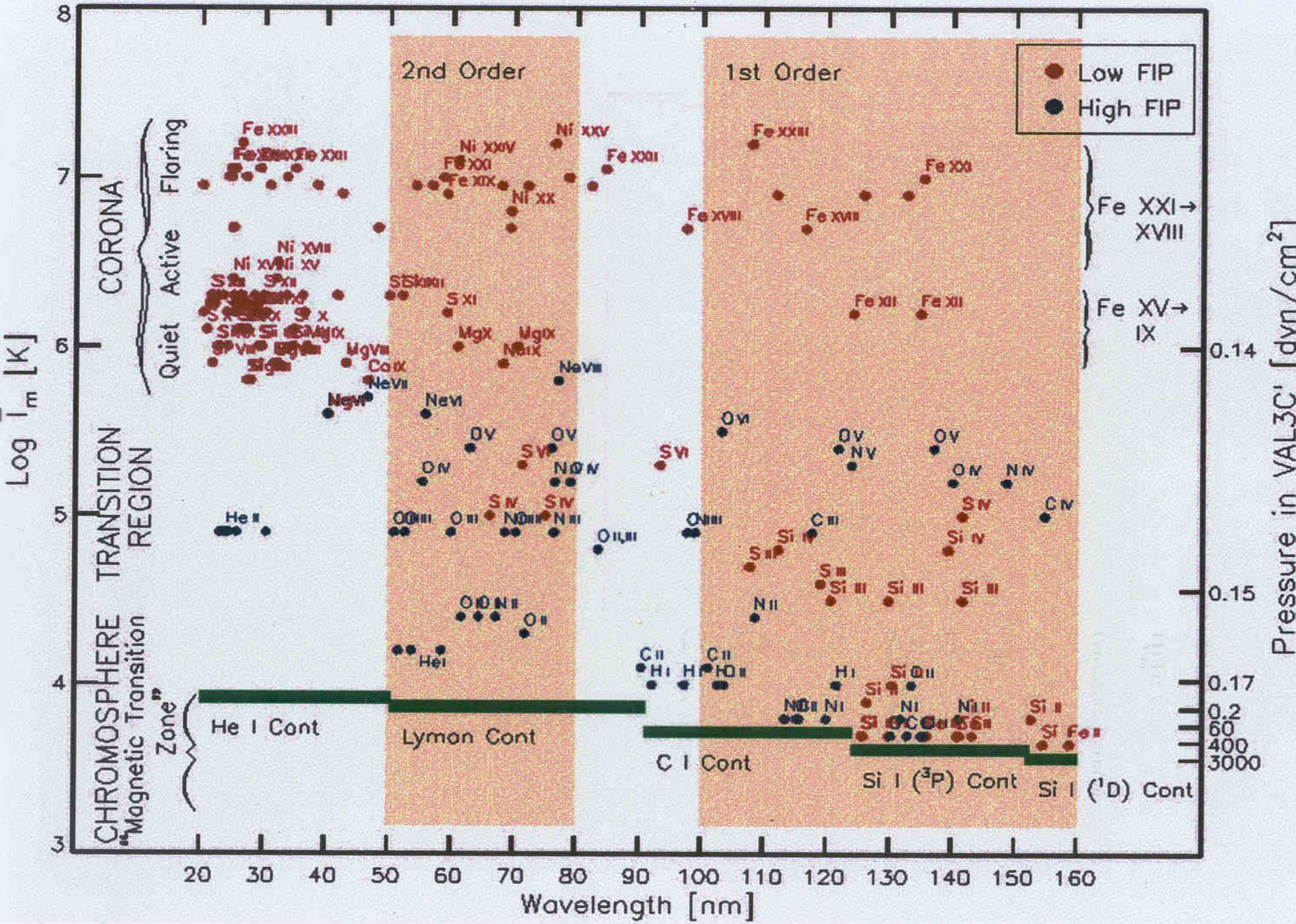

2nd Order
1st Order
Low FIP
High FIP
CORONA
Flaring
Active
Quiet
TRANSITION REGION
CHROMOSPHERE
"Magnetic Transition Zone"
Fe XXI→ XVIII
Fe XV→ IX
He I Cont
Lyman Cont
C I Cont
Si I (^{3}P) Cont
Si I (^{1}D) Cont
Log $\bar{T}_m$ [K]
Wavelength [nm]
Pressure in VAL3C' [dyn/cm^2]
0.14
0.15
0.17
0.2
60
400
3000
20 30 40 50 60 70 80 90 100 110 120 130 140 150 160
3 4 5 6 7 8

Doppler flows

- $\Delta\lambda / \lambda = v / c$
- Hires spectroscopes can resolve 1- 2 km/s

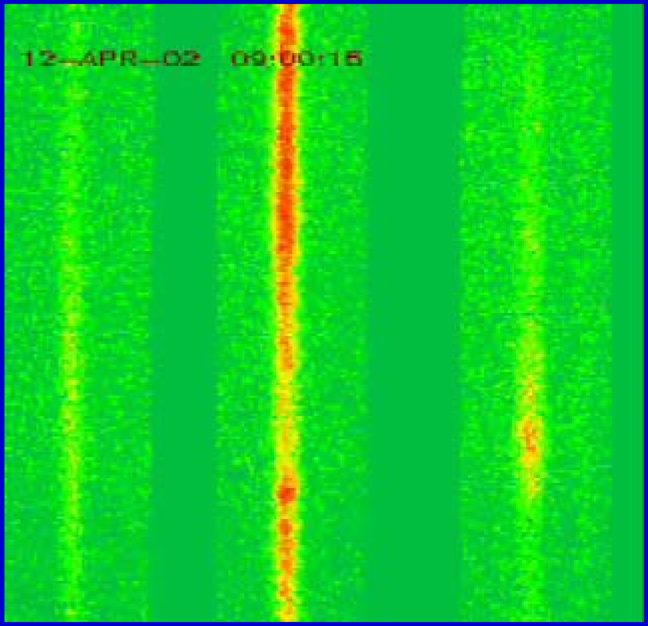

Si III Ca X Fe IXX

EUV Spectroscopy

Line emission

$$P(\lambda) = \int \frac{hc}{\lambda} \quad A_{ul} \quad N_u \quad dV$$

$\boldsymbol{A}_{ul}$ upper/lower level transition probabability

$$Nu = \frac{Nu(X^{+p})}{N(X^{+p})} \quad \frac{Nu(X^{+p})}{N(X)} \quad \frac{N(X)}{N(H)} \quad \frac{N(H)}{Ne} \quad Ne$$

excited level population | degree of ionization | elemental abundance | hydrogen abundance

Chianti
ADAS
NIST

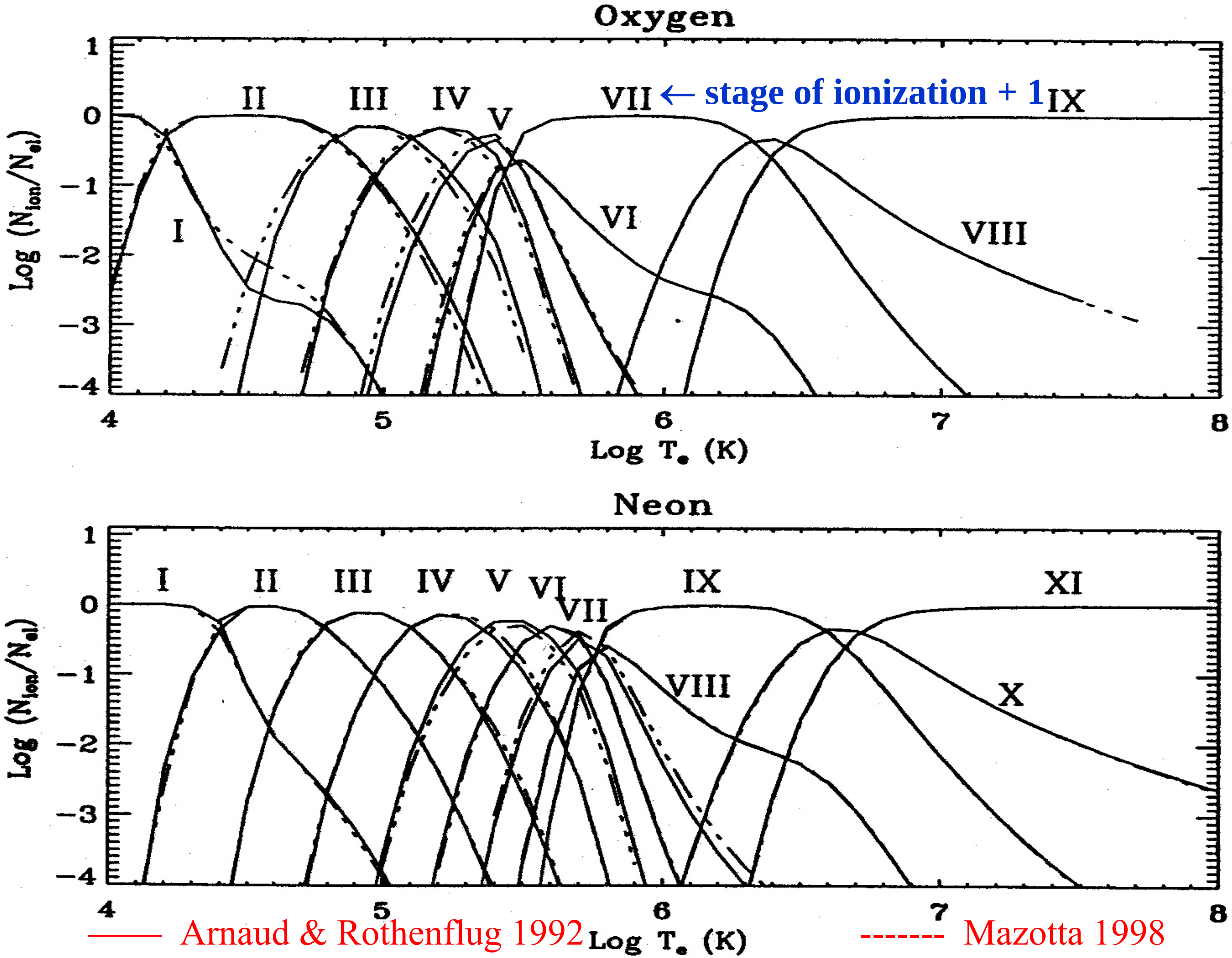
Oxygen
← stage of ionization + 1
I
II
III
IV
V
VI
VII
VIII
IX
Log (N_{ion}/N_{el})
Log T_e (K)
Neon
I
II
III
IV
V
VI
VII
VIII
IX
X
XI
Log (N_{ion}/N_{el})
Log T_e (K)
Arnaud & Rothenflug 1992
Mazotta 1998

radiative excitation:

- optical pumping

  some atomic systems have transitions into the ground state that coincide with strong lines

  heating of the geo-corona

- self-reversal

Gouttebroze 1978

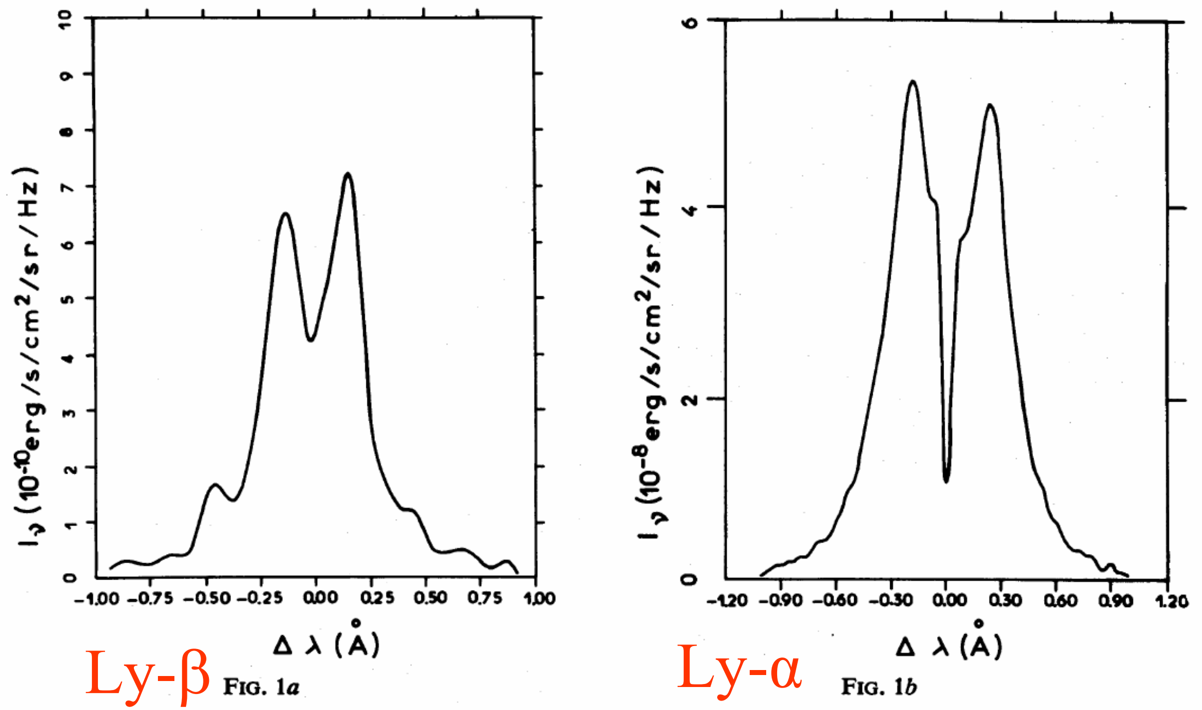

FIG. 1.—Observed profiles at the center of the solar disk. (*a*) Lβ. (*b*) Lα.

Line shape

- Optically thin emission lines are Gaussians

- emission profile $\Psi(\lambda)$

$$\Psi(\lambda) = \Psi(\lambda)_{nat} * \Psi(\lambda)_{coll} * \Psi(\lambda)_{th} * \Psi(\lambda)_{NT}$$

- $\Delta\lambda_D = \lambda_0/c\ (2kT/m + \xi^2)^{1/2}$

  ξ non-thermal velocity (turbulence)

Line ratios

$$P_{ul}(\lambda) \approx N_e^{\,2}$$

allowed transitions:

electric dipol transitions

$$\Delta l = \pm 1$$
$$\Delta m = 0, \pm 1$$
$$\Delta s = 0$$

$$P_{ul}(\lambda) \approx N_e$$

metastable levels:
M1, E2, M2, ...
intersystem transition

N_e diagnostics

T_e diagnostics

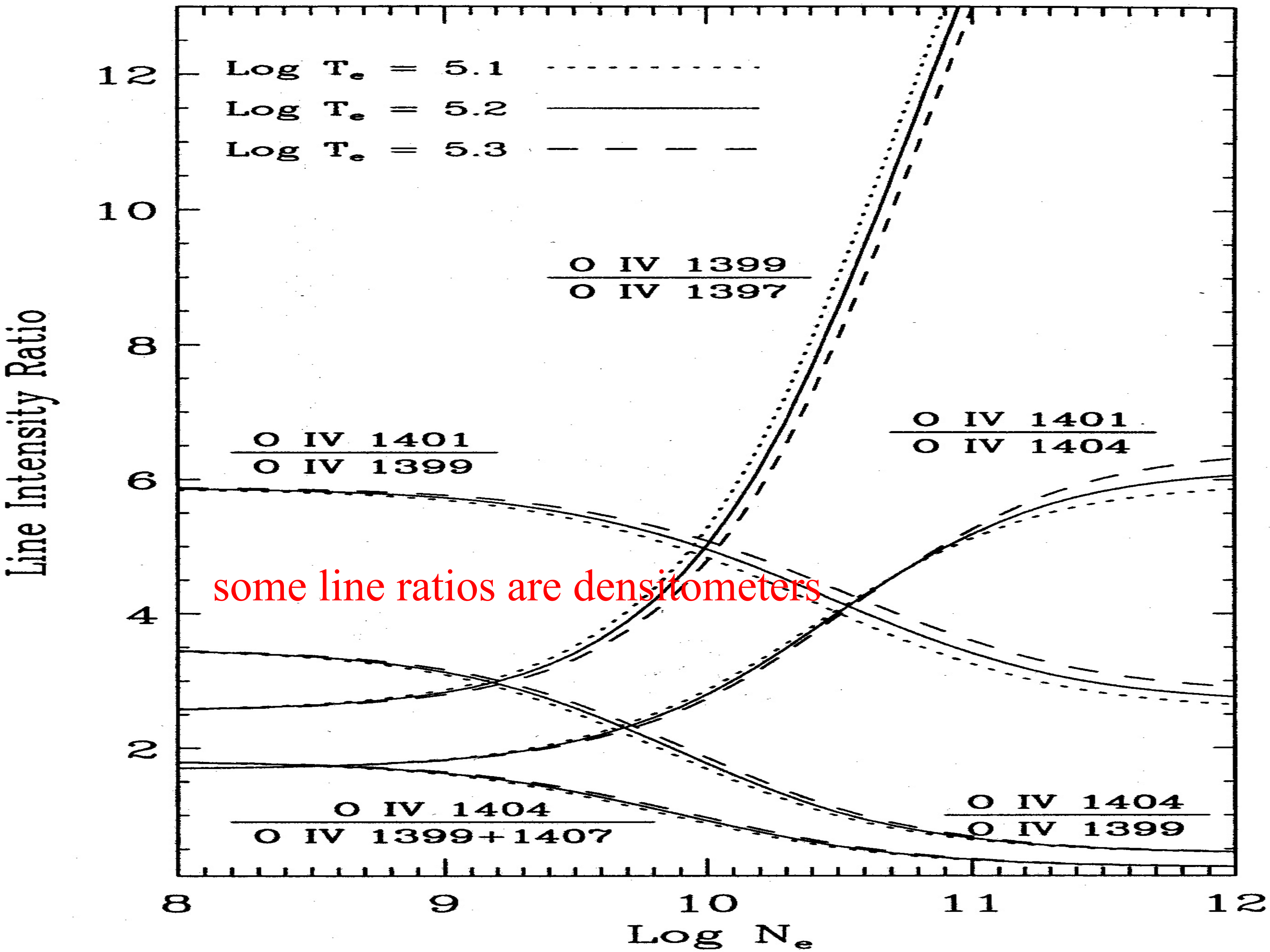

Log T_e = 5.1
Log T_e = 5.2
Log T_e = 5.3
O IV 1399 / O IV 1397
O IV 1401 / O IV 1399
O IV 1401 / O IV 1404
O IV 1404 / O IV 1399+1407
O IV 1404 / O IV 1399
some line ratios are densitometers
Line Intensity Ratio
Log N_e

Historical overview

- 1950 Bragg-crystal spectrometers
- 1962 OSO armada
- 1973 Apollo Telescope Mount
- 1975 HRTS, 8 rocket flights
- 1985 HRTS, Spacelab 2
- 1996 SOHO-CDS
- 1996 SOHO-SUMER
- 2006 Hinode-EIS
- 2012 IRIS
- 2018 SO SPICE

Performance characteristic

Coronal Diagnostic Spectrograph
Solar Ultraviolet Measurement of Emitted Radiation
EUV Imaging Spectrograph

	CDS	SUMER	EIS
wavelegth range, Å	308-381 (NI)	790-1608 (1)	180 - 204 (A)
	513-633	465-804 (2)	240 - 290 (B)
	151-221 (GI)		
	256-338		
	393-493		
	656-785		
spatial resolution / ″	4 - 8	1.2	1
spectral ″ / km/s	10	2	2-3
temporal ″ / s	10	10	1

Instrumental aspects

- Spectroscope:
  - telescope
  - slit
  - dispersive element
  - 2D detector
- infrastructure
  - to bring the instrument into space
  - to bring the data back to Earth

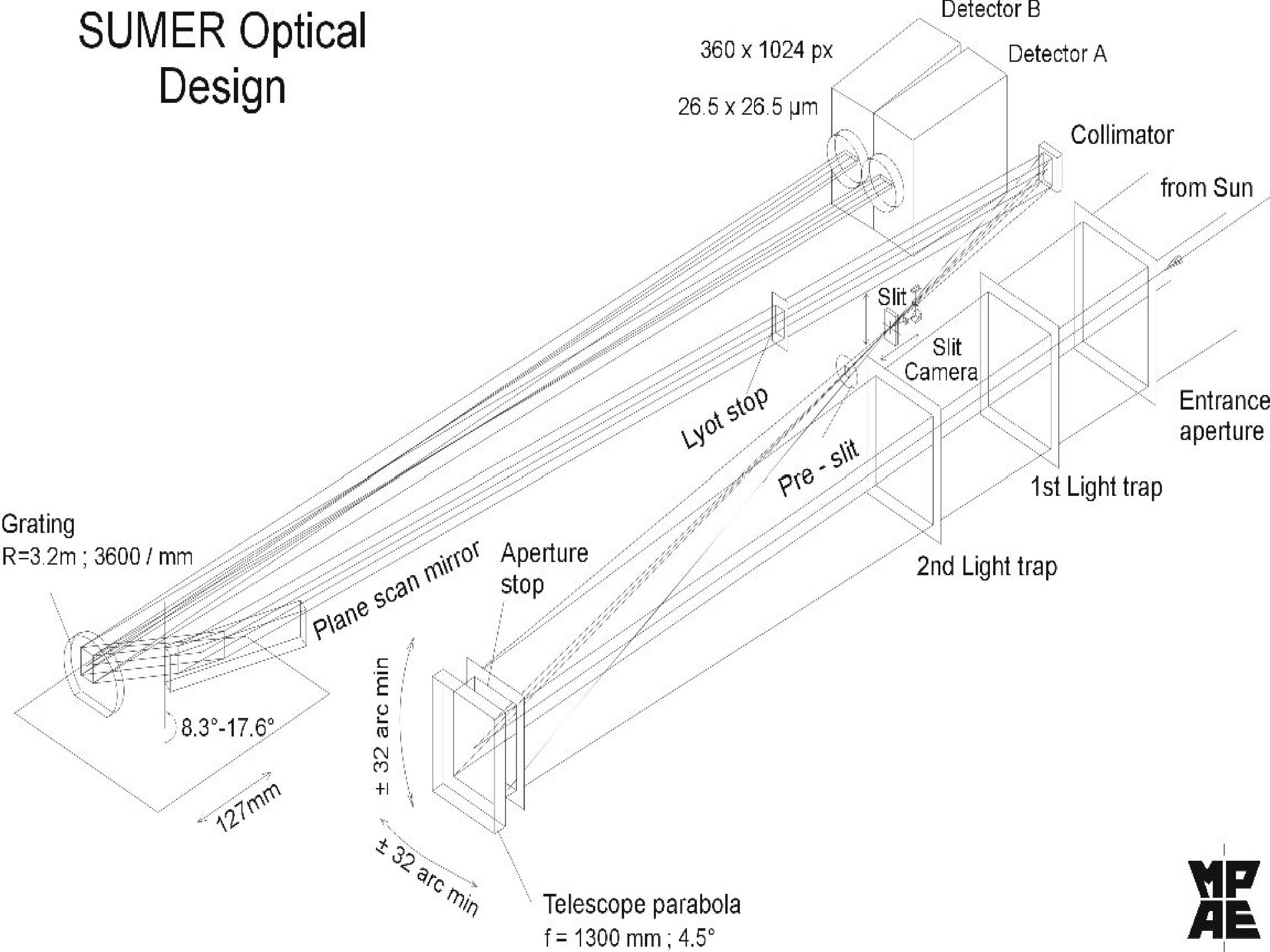

SUMER Optical Design
Detector B
Detector A
360 x 1024 px
26.5 x 26.5 µm
Collimator
from Sun
Slit
Slit Camera
Entrance aperture
Lyot stop
Pre - slit
1st Light trap
2nd Light trap
Grating
R=3.2m ; 3600 / mm
Plane scan mirror
Aperture stop
8.3°-17.6°
127mm
± 32 arc min
± 32 arc min
Telescope parabola
f = 1300 mm ; 4.5°

Telescope primary mirror

- size determines spatial resolution, λ/D
- size ~ photon input ⇒ temporal resolution
- figure defines PSF
- micro roughness defines scattered light level
- needs pointing mechanism
- optical surface:
  - $\lambda > 120$ nm ⇒ Al/MgF_2
  - $\lambda > 50$ nm ⇒ Si C
  - $\lambda < 50$ nm grazing incidence (Wolter) or multilayer coating

Telescope slit

- slit width limits photon input
- slit width limits spectral resolution
- slit: loss of >99% of photons
  - slitless spectroscopes (strong lines, filters)
  - slot spectroscopes (wide slit)
  - raster scans
  - drift scans (low temporal resolution)

Telescope collimator

- Makes parallel light (classical design)
- defines magnification (pixel adjustment)
- folds the light beam (compactness)

Spectroscope grating

- Bragg crystal systems
- holographic gratings
- ruled gratings
- variable line space technique (TVLS)
  - future 2 reflection designs

Instrument detector(s)

- Films
- CCDs
  - back-illuminated CCDs
  - intensified CCDs
- MCP detectors
  - multianode systems (MAMA)
  - time delay systems (XDL)
- APS sensors
- BOLD detectors

Telemetry issues

16 bit pixels	dynamical range
1 k x 1k	small and numerous
10 s	good time resolution

Example SUMER: $\frac{16 \text{ bit/px} \times 400\,000 \text{ bit}}{10 \text{ s}}$ ≈500 kbit/s

Data selection	windows, binning
Data compression	sqrt, JPEG, MPEG
Data reduction	moments

Sunspot onbserved on Mar 18, 1999

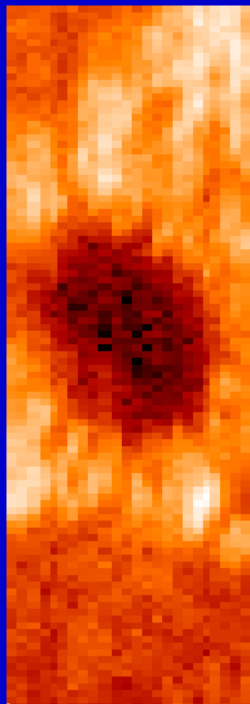

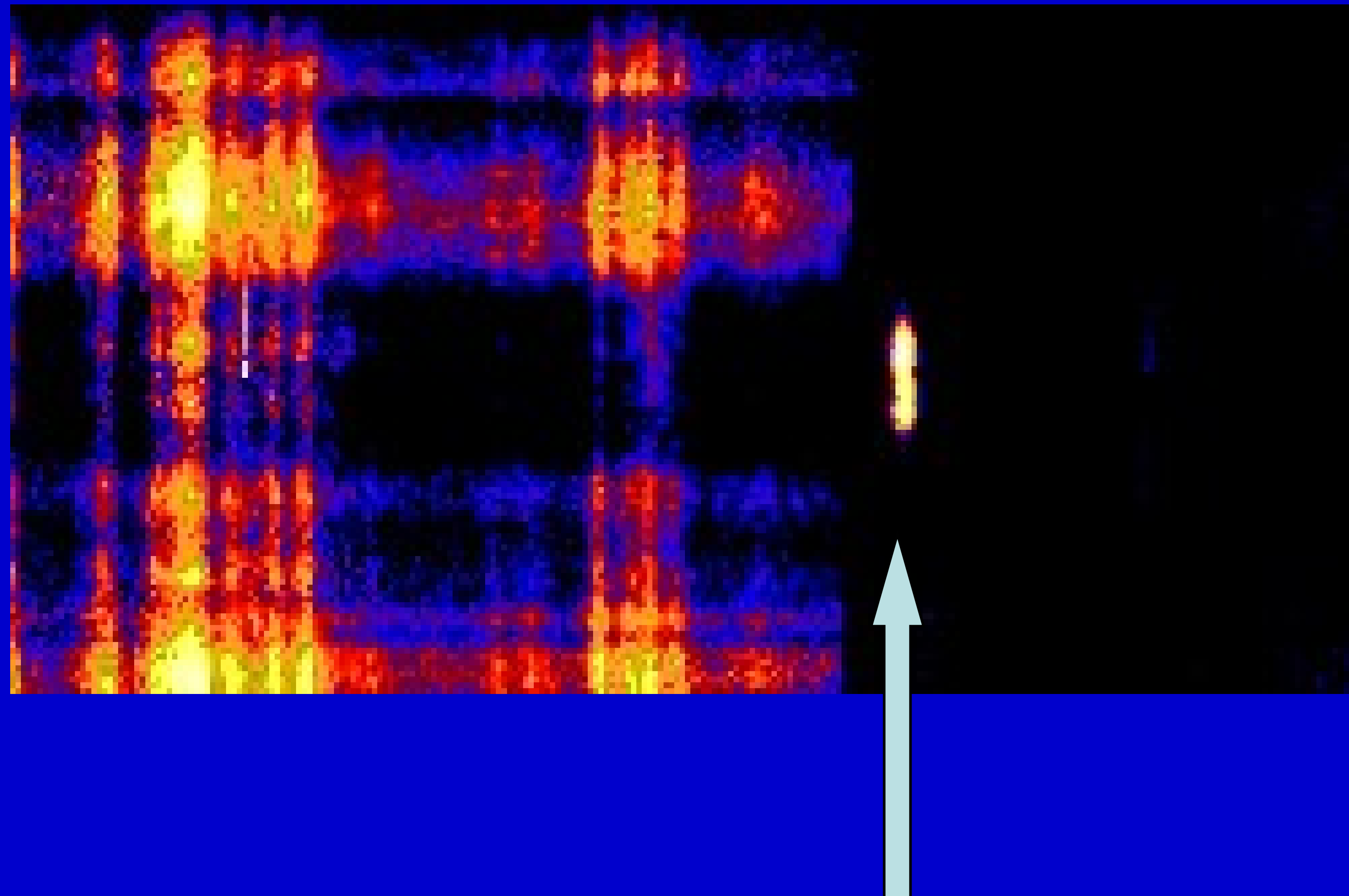

Raster scan in the continuum @ 1478 Å

Spectrum around 1163 Å with strong H_2 fluorescence emision

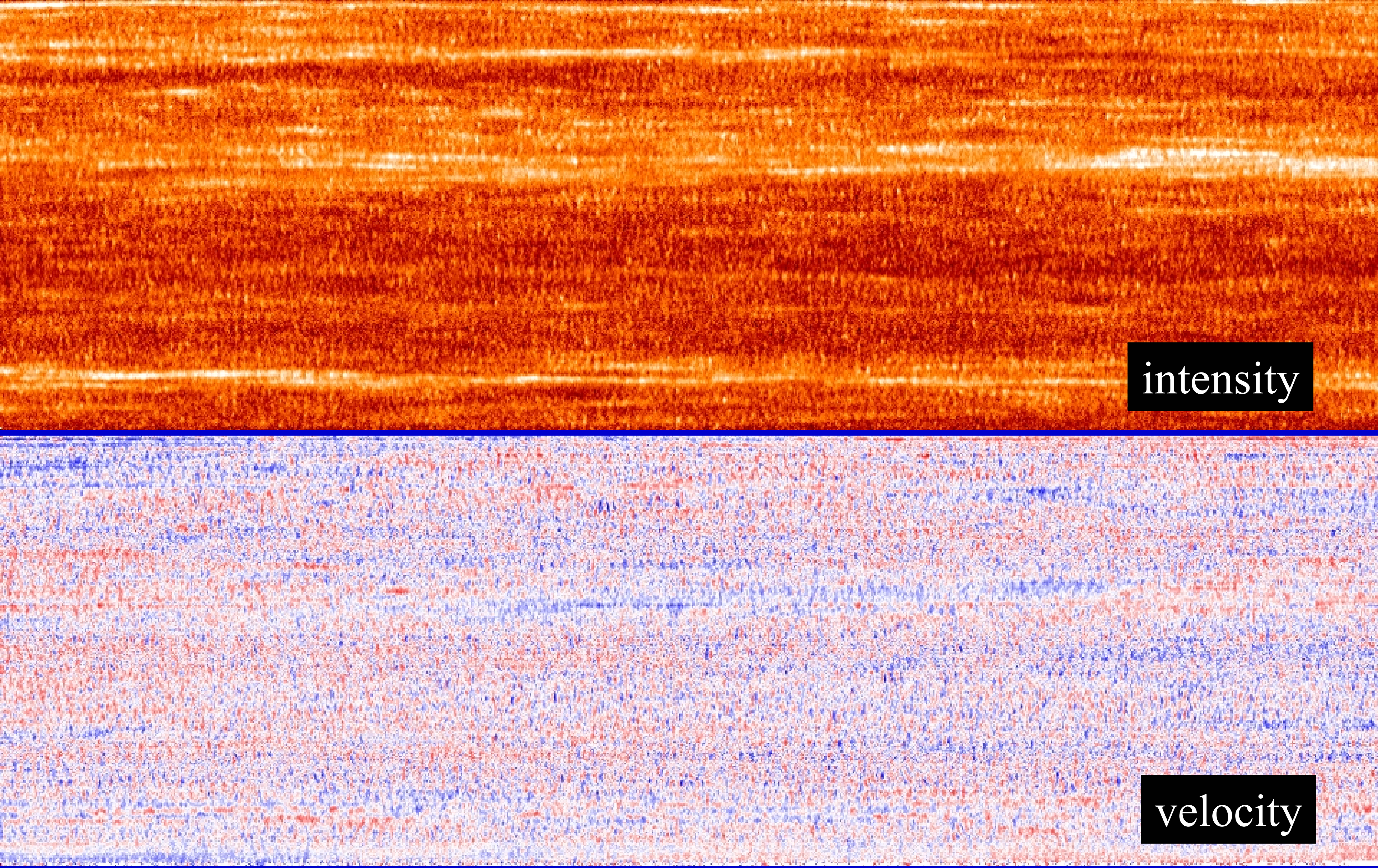

Drift scan (x-t map) over 9 hours

Si II 130.9 nm

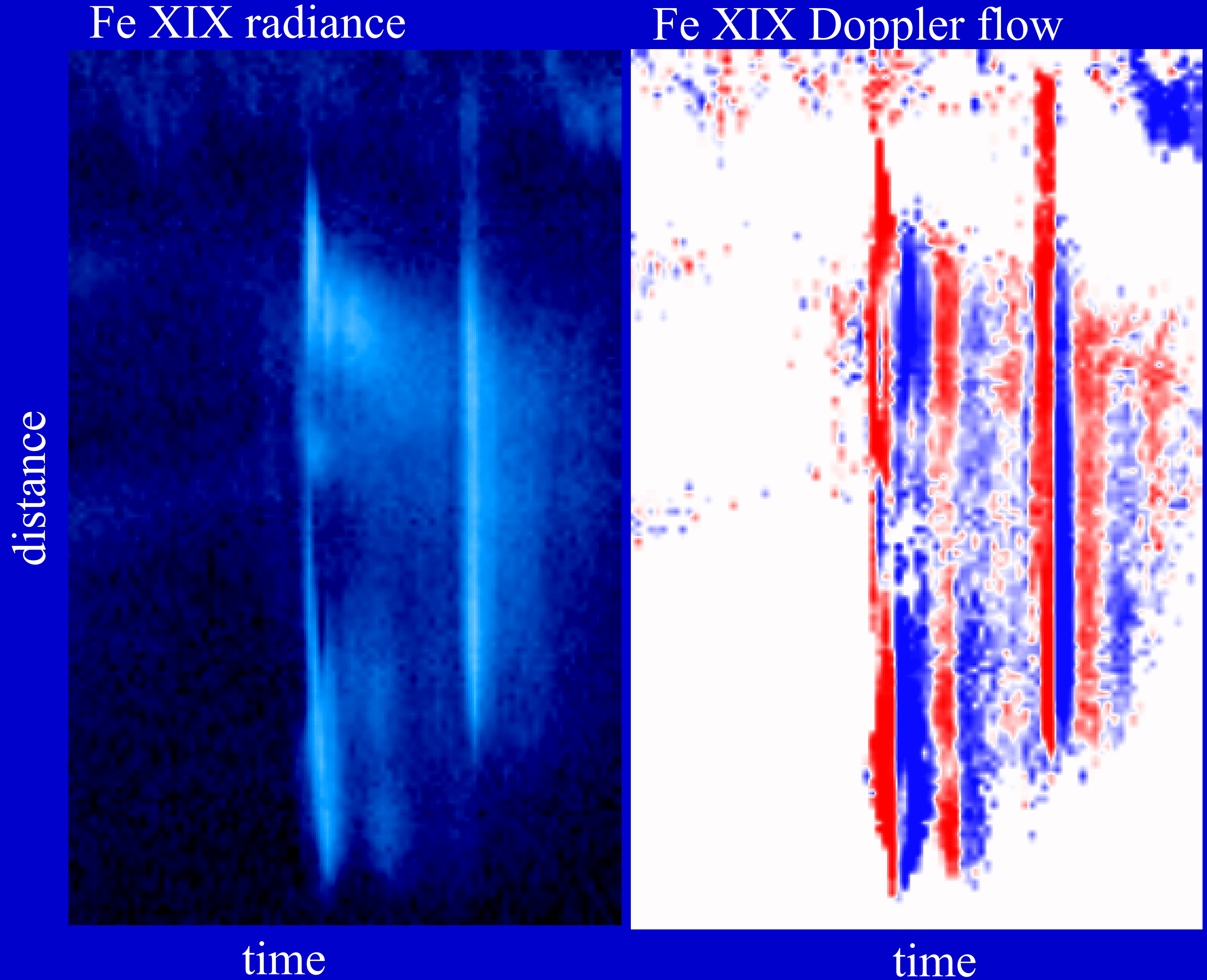

28 Sep 2000

Solar and stellar EUV spectra

Sun @ 130 nm (black) / α Cen A (red)

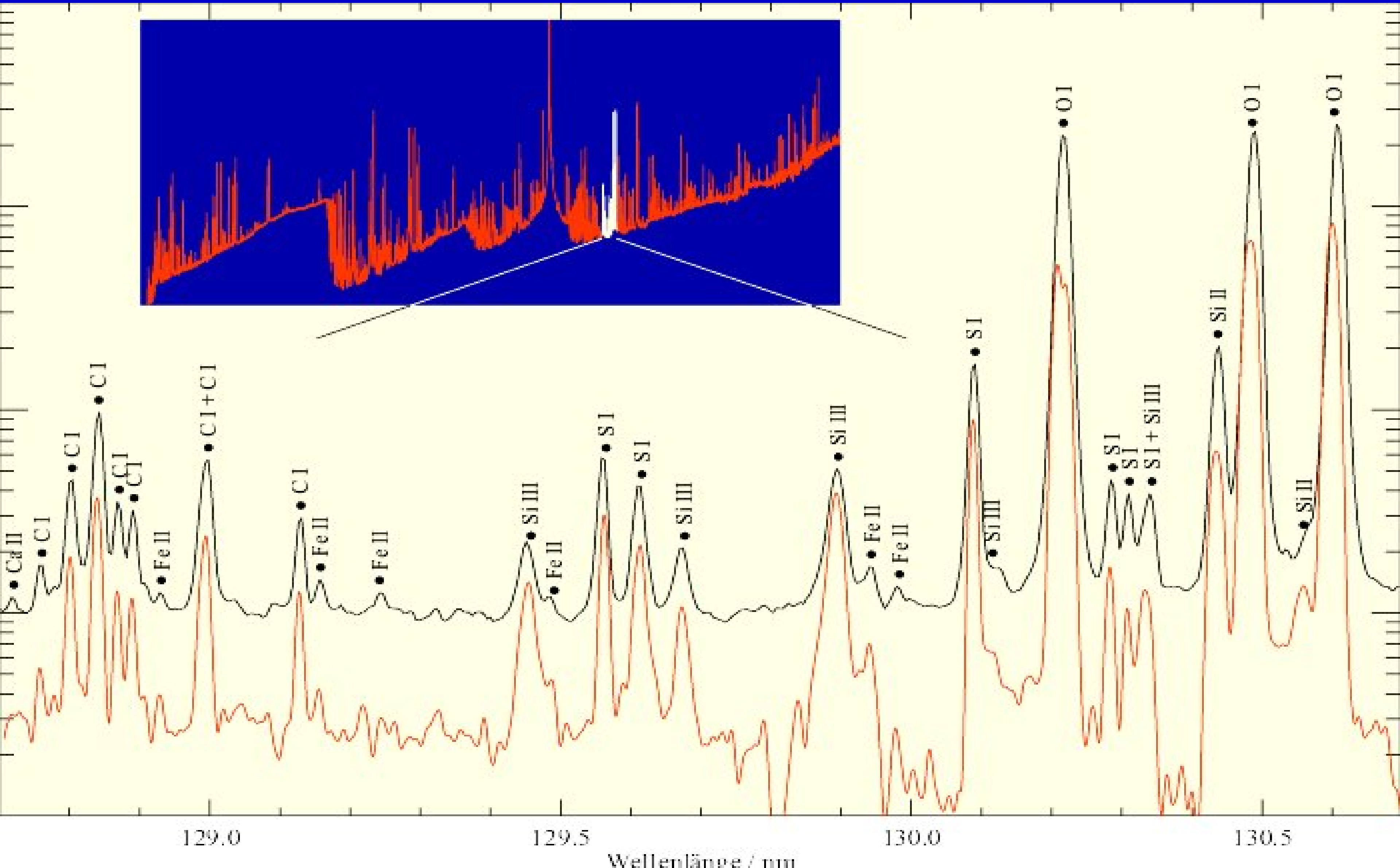

Full Sun raster scan
in C III 97.7 nm

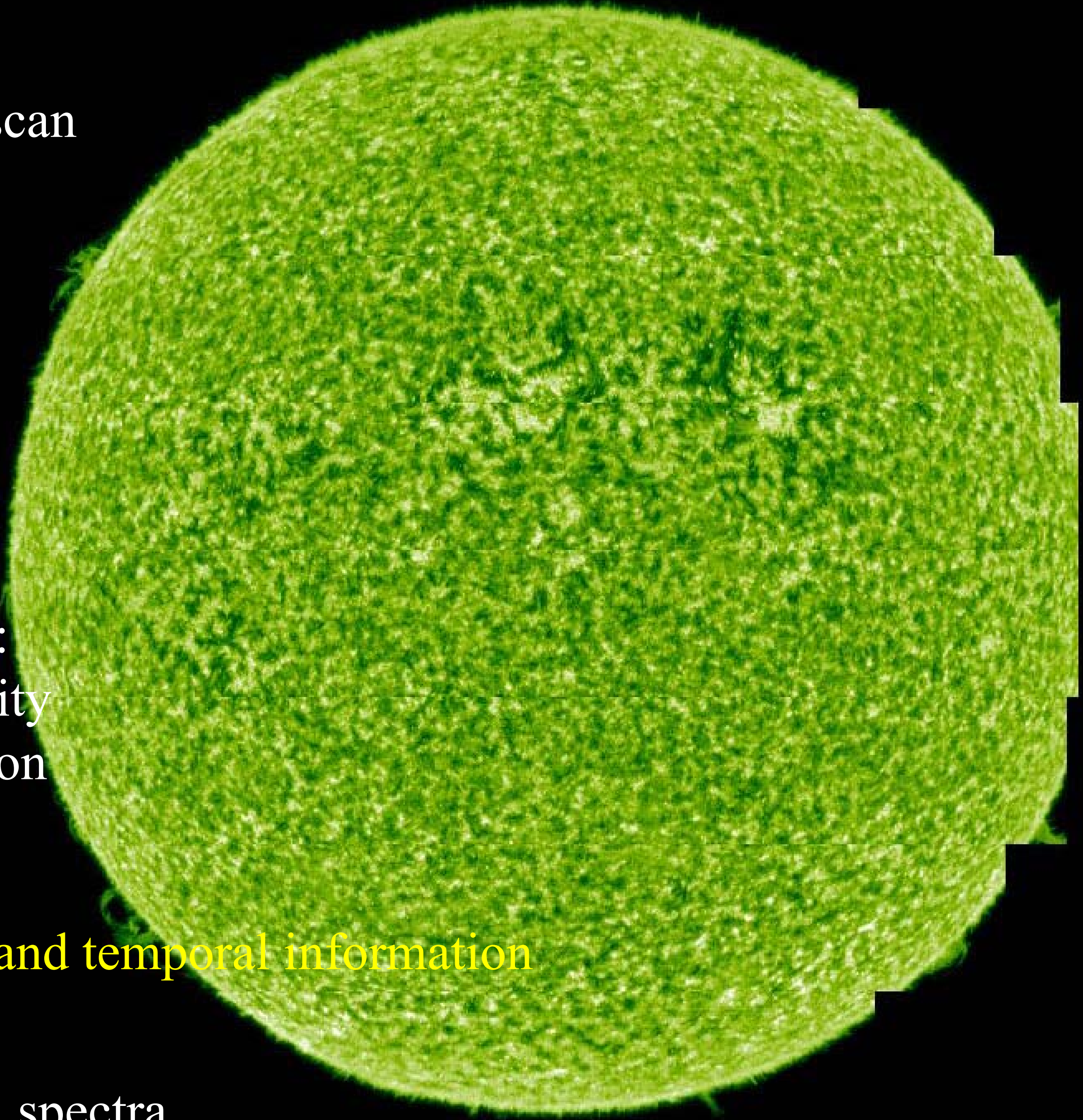

spectroscopy basics:
- line-of-sight velocity
- „in situ“ information
- spectrally clean
- waste of photons
- mixture of spatial and temporal information

25 hours
12338 individual spectra

Outlook

- SUMER and CDS still in operation
- HINODE EIS
- IRIS
- Solar orbiter SPICE
- SOLAR C

Coronagraphy

Schwenn 2006

The solar corona: the 3 main types

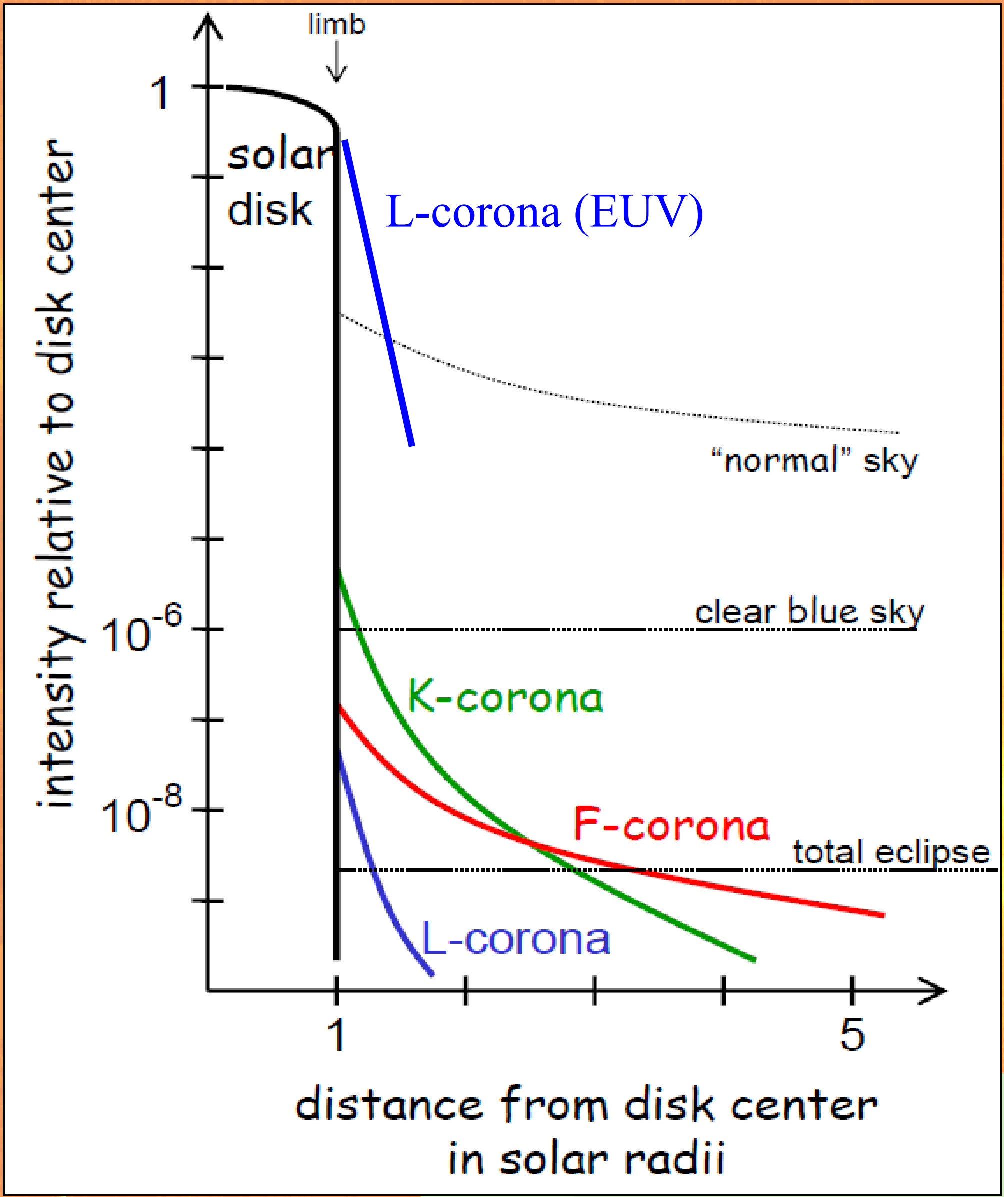

(K) continuum corona

- no absorption lines
- polarised:
  free electron scattering

(F) Fraunhofer corona

- absorption lines visible
- not polarized:
  dusk scattering
- Zodiac light…

(L) Line corona

- emission lines:
  e.g.: "green coronal line"
- *emission of atoms / ions:*
  new elements?
  helium, "coronium"

Diffraction limit of spatial resolution

Diffraction limit for externally occulted coronagraph

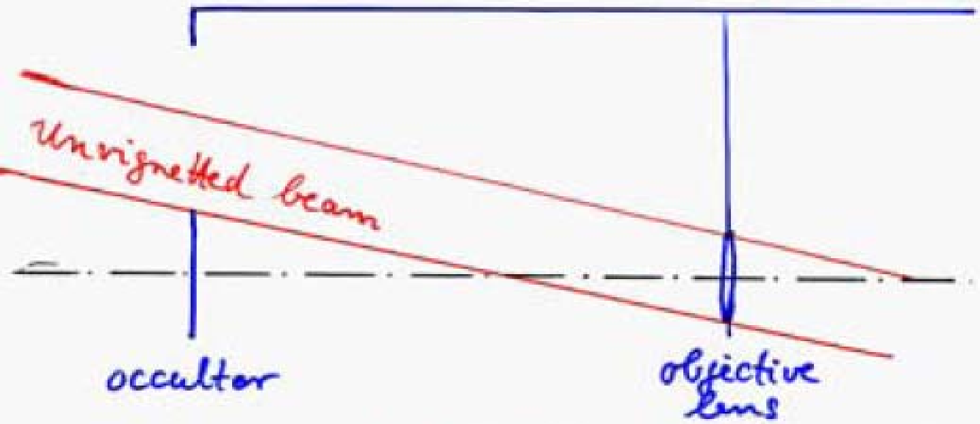

diffraction limit set by objective lens

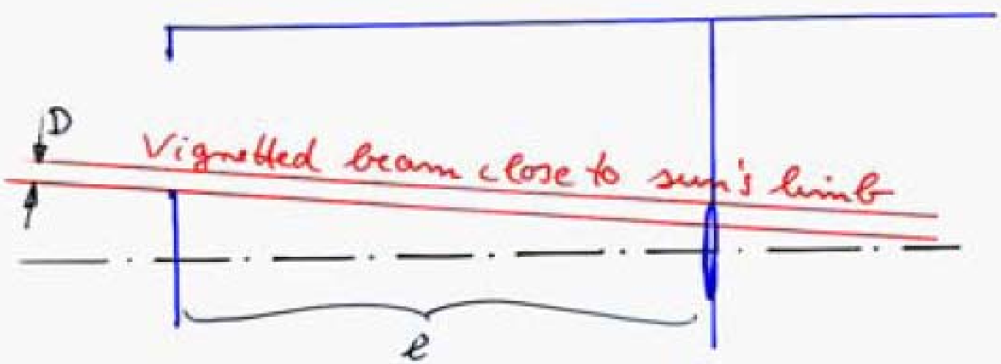

for the inner field of view, the diffraction limit is set by distance and size of external occultor.

$$\sin \varphi_{min} = 1.22 \cdot \frac{\lambda}{D}$$

The problem with external occultation in coronagraphs of limited size:
For regions close to the limb there is substantial vignetting.

External occulter systems are perfect to view the outer corona, but suffer from vignetting near the inner edge (loss of spatial resolution).

Wait for solar eclipse!
Formation flying spacecraft!

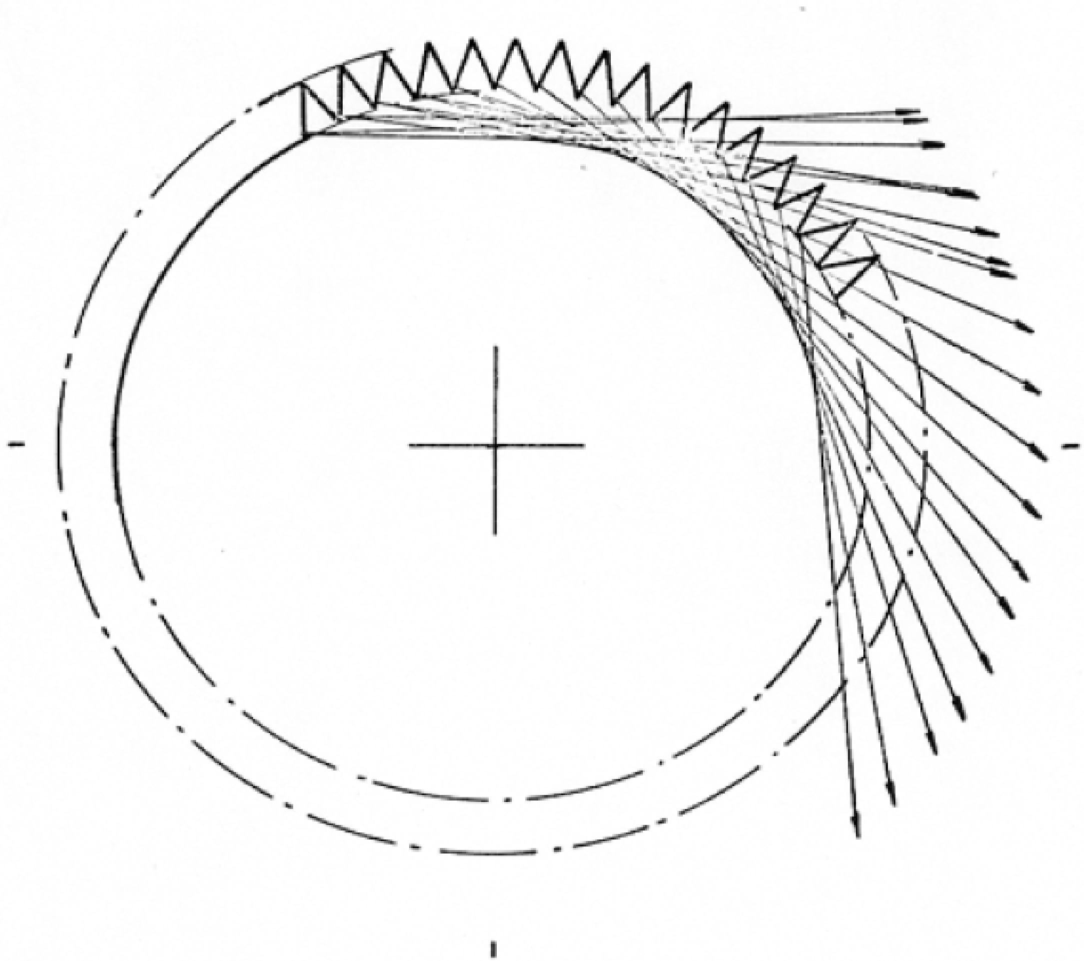

Fig. 7. Direction of diffracted parallel light from the periphery of a sawtooth disk or serrated edge (from Purcell and Koomen, 1962). The incident beam is perpendicular to the plane of the figure and the directions of the diffracted rays are shown in projection on the plane of the figure, so they do not reach the optical system of a coronagraph.

Straylight reduction by a cerrated occulter:
diffracted rays have a component to leave the optical system

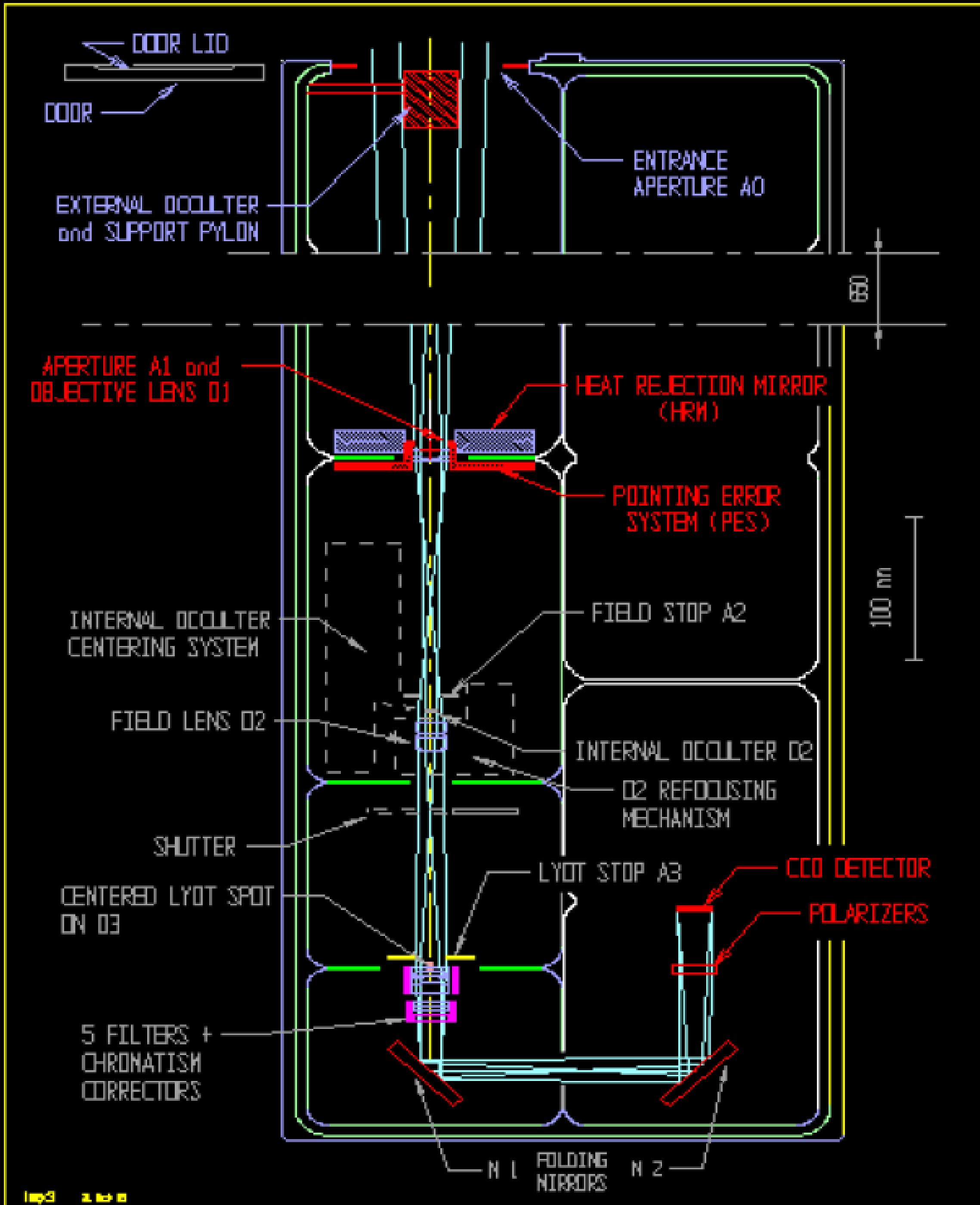

LASCO C2

The problem of internally occulted systems:

the full illumination leads to

- straylight of the aperture and the main mirror

- heat

EUV Spectroscopy

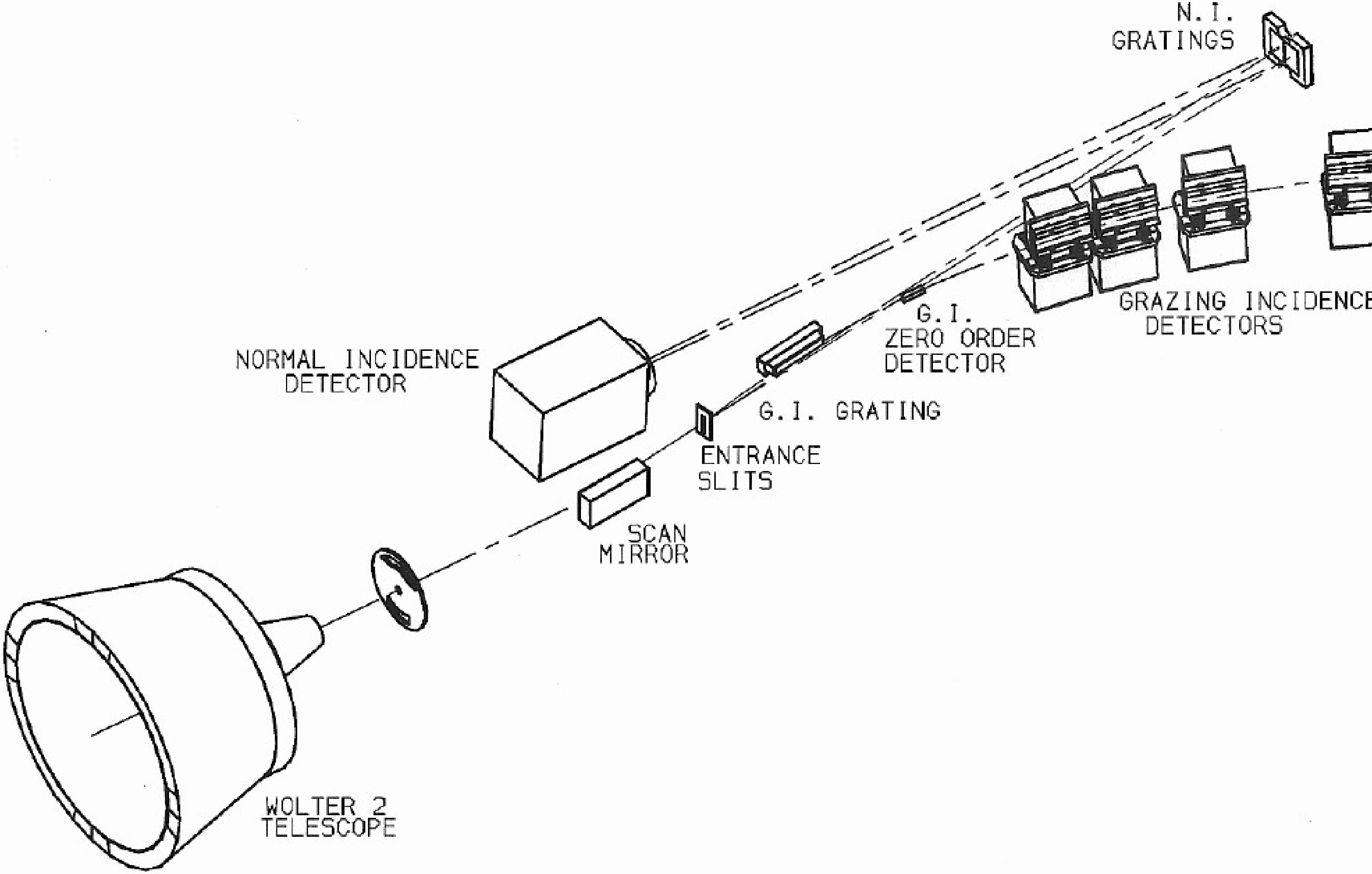
N.I.
GRATINGS
GRAZING INCIDENCE
DETECTORS
G.I.
ZERO ORDER
DETECTOR
NORMAL INCIDENCE
DETECTOR
G.I. GRATING
ENTRANCE
SLITS
SCAN
MIRROR
WOLTER 2
TELESCOPE

CDS OPTICS